Published in final edited form as:
J Cereb Blood Flow Metab. 2008 June ; 28(6): 1165–1174. doi:10.1038/jcbfm.2008.5.

Brain Redox Imaging Using Blood Brain Barrier Permeable Nitroxide MRI Contrast Agent

Fuminori Hyodo[1], **Kai-Hsiang Chuang**[2], **Artem G Goloshevsky**[2], **Agnieszka Sulima**[3], **Gary L. Griffiths**[3], **James B Mitchell**[1], **Alan P Koretsky**[2], and **Murali C. Krishna**[1,*]

[1]Radiation Biology Branch, Center for Cancer Research, National Cancer Institute, NIH, Bethesda, MD, USA

[2]Laboratory of Functional and Molecular Imaging, National Institute of Neurological Disorders and Stroke, NIH, Bethesda, MD, USA

[3]Imaging Probe Development Center, National Heart, Lung and Blood Institute, NIH, Bethesda, MD, USA

Abstract

Reactive oxygen species (ROS) and compromised antioxidant defense may contribute to brain disorders such as stroke, amyotrophic lateral sclerosis, etc. Nitroxides are redox-sensitive paramagnetic contrast agents and antioxidants. The ability of a blood brain barrier (BBB) permeable nitroxide, methoxycarbonyl-2,2,5,5-tetramethylpyrrolidine-1-oxyl (MC-P), as an MRI contrast agent for brain tissue redox imaging was tested. MC-P relaxation in the rodent brain was quantified by MRI using a fast Look-Locker (LL) T_1 mapping sequence. MRI signal intensity in the cerebral cortex and thalamus increased up to 50 % after MC-P injection, but only (2.7 %) increase when a BBB-impermeable nitroxide, 3-carboxy PROXYL was used. The maximum concentration in thalamus and cerebral cortex after MC-P injection was calculated to be 1.9 ± 0.35 mM and 3.0 ± 0.50 mM. These values were consistent with the ex-vivo data of brain tissue and blood concentration obtained by electron paramagnetic resonance (EPR) spectroscopy. Also, reduction rates of MC-P were significantly decreased after reperfusion post transient middle cerebral artery occlusion (MCAO), a condition associated with changes in redox status resulting from oxidative damage. These results demonstrate use of BBB permeable nitroxides as MRI contrast agents and antioxidants to evaluate the role of ROS in neurological diseases.

Keywords

redox; blood brain permeable contrast agent; nitroxide; MRI; free radical

Introduction

Increased reactive oxygen species (ROS) and decreased antioxidant defense may contribute to numerous brain disorders such as stroke, amyotrophic lateral sclerosis, Parkinson's disease and Alzheimer's disease (Halliwell 2006; Huang *et al* 2001; Mariani *et al* 2005; Muir *et al* 2006; Raichle and Mintun 2006; Zimmermann *et al* 2004). Non-invasive assessment of oxidative stress is therefore useful to monitor the role of ROS in brain disorders. To image the ROS in vivo, nitroxide compounds have been utilized as redox

[*]*Correspondence to:* Murali C. Krishna, Building 10, Room B3B69, NIH, Bethesda, MD 20892-1002. Tel: 301-496-7511. Fax: 301-480-2238. murali@helix.nih.gov.

sensitive contrast agent by electron paramagnetic resonance (EPR) imaging (He *et al* 2002; Kuppusamy *et al* 2002; Yamada *et al* 2002).

Nitroxides are nontoxic stable organic free radicals having a single unpaired electron and therefore capable of providing MRI contrast via shortening the longitudinal relaxation time (T_1). Though nitroxides have a lower relaxivity compared to conventional T_1 contrast agents such as Gd^{3+}-complexes, the volume distribution of nitroxides is significantly greater due to better cell permeability (Hahn *et al* 1992; Samuni *et al* 2001). The rapid bio-reduction from paramagnetic nitroxides to the corresponding diamagnetic hydroxylamines has compromised their utility as contrast agents (Keana and Pou 1985). The combination of relatively low relaxitivity and short life times precluded the use of nitroxides as MRI contrast agents. However, with the improved sensitivity of MRI and shift to higher magnetic fields, recent work has begun to investigate whether the reduction of nitroxides might be useful in obtaining information pertaining to tissue redox status. (Hyodo *et al* 2006; Matsumoto *et al* 2006). Nitroxides can be reduced to the corresponding hydroxylamines by reductants such as ascorbate (Fig. 1). Nitroxides were investigated to be used as antioxidants and radioprotectors in preclinical cancer research (Erker *et al* 2005; Hahn *et al* 1997; Krishna *et al* 1996a; Liaw *et al* 2005; Metz *et al* 2004). In *in vivo* studies, the ratio of the nitroxide/hydroxylamine has been shown to be dependent on the redox status of the tissue (Hahn *et al* 2000; Kuppusamy *et al* 1996; Kuppusamy *et al* 2002). These observations suggest that nitroxides participate in cellular redox reactions and that their relative levels may be indicative of the cellular redox status.

One of the nitroxides, methoxycarbonyl-2,2,5,5-tetramethylpyrrolidine-1-oxyl (MC-P; figure 1), has been used as a contrast agent for brain imaging in electron paramagnetic resonance (EPR) imaging experiments (Anzai *et al* 2006; Lee *et al* 2004; Sano *et al* 1997; Yokoyama *et al* 2002). Anzai et al. (Anzai *et al* 2003) confirmed that the nitroxide, MC-P, after iv injection, accumulated in the brain tissue as evidenced by autoradiography. These findings suggest that MC-P can pass through the BBB and give T_1 contrast in brain tissue. Previously we demonstrated that nitroxides are useful contrast agents for monitoring tissue redox status using MRI with improved spatial and temporal resolutions compared to EPR imaging (Hyodo *et al* 2006; Matsumoto *et al* 2006). Therefore, MC-P can be used as a BBB permeable MRI contrast agent that can participate in redox reactions. The middle cerebral artery occlusion (MCAO) in rats is generally accepted as a standard model of focal cerebral ischemia (Koizumi *et al* 1986; Longa *et al* 1989; Nagasawa and Kogure 1989). After periods of ischemia, upon reperfusion with oxygenated buffer solutions, a burst of ROS have been shown to be generated with a propensity to inflict oxidative damage and also alter the tissue redox status and shift the equilibrium shown in Figure 1 towards left. To demonstrate the possibility of MC-P to brain redox imaging in neurological disease model, rat transient MCAO model was employed. Furthermore, T_1 mapping has the potential to quantify the tissue concentration of the contrast agent with the knowledge of the relaxivity of the agent used. Chuang et al. (Chuang and Koretsky 2006) reported fast T_1 mapping based on the Look-Locker (LL) sequence that can significantly reduce scanning time without sacrificing accuracy. This has been shown to have almost the same efficiency as the spin echo inversion recovery method in terms of the SNR per unit time (Crawley and Henkelman 1988). Using the LL sequence, we used MRI to study the pharmacokinetics of MC-P concentration in the brain by monitoring T_1 changes before and after MC-P injection. T_1 changes were readily detected throughout the brain at a well-tolerated dose of MC-P. Maximum T_1 reduction occurred at about 3 min after injection and returned to control by 15 min. A BBB-impermeable 3CxP did not change T_1 in the brain. Estimation of the concentration of MC-P using in vitro relaxivities agreed with EPR results from extracted tissue. The results indicate that MC-P goes into the brain and causes reduction of T_1. In addition, reduction rate of MC-P was significantly decreased in the infarct region of brain after ischemia followed by

reperfusion compared to same region of sham group. This opens the possibility of using this agent for MRI study of brain redox status and the changes under pathological conditions.

MATERIALS AND METHODS

Chemicals

Methoxycarbonyl-2,2,5,5-tetramethylpyrrolidine-1-oxyl (MC-P) was purchased from Columbia Advanced Science, LC (Maryland, USA). 3-carboxy-2,2,5,5,5-tetramethylpyrrolidine-1-oxyl; 3CxP) was purchased from Sigma-Aldrich Chemical Co. (St. Louis, MO). Deionized water was used for all experiments. Potassium chloride (KCl) was purchased from Hospira inc. (Lake Forest, IL, USA). Other materials used were of analytical grade.

Animals

Male Wistar rats were supplied by the Frederick Cancer Research Center, Animal Production (Frederick, MD). The rats were 6–7 weeks of age at the time of experiments and were housed three per cage in climate controlled, circadian rhythm-adjusted rooms and were allowed food and water ad libitum. All *in vivo* experiments were carried out in compliance with the Guide for the Care and Use of Laboratory Animal Resources (1996), National Research Council, and approved by the National Cancer Institute Animal Care and Use Committee.

MRI and Pulse sequence

MRI measurements were performed an at 4.7 T scanner controlled with ParaVision® 3.0.1 (Bruker BioSpin MRI GmbH, Rheinstetten, Germany). A series of T_1-weighted spoiled gradient echo (SPGR; TR = 75 ms, TE = 3 ms, flip-angle (FA) = 45°, N_{EX} = 2) was employed to observe T_1 effects. The scan time for an image set (which included 6 slices) by the SPGR sequence was 20 s. Other imaging parameters were as follows: image resolution was 256 × 128 zero-filled to 256 × 256 (0.125 mm resolution), FOV was 3.2 × 3.2 cm, slice thickness was 2.0 mm and 0.2 mm gap. Number of slices was 6.

For quantification of the dynamic change of T_1 and to estimate the concentration of the contrast agent, three MC-P injected rats were scanned by a fast LL T_1 mapping sequence (Chuang and Koretsky 2006). After adjusting higher order shimming, echo spacing, echo symmetry, and B_0 compensation, multi-slice LL data were acquired by segmented gradient-echo echo planar imaging (EPI) with TR = 10 s, TE 6.7 ms, FA = 20°, acquisition interval = 400 ms, and number of LL time points = 20. To avoid resolution blurring due to the T_2* of the brain, a bandwidth of 250k Hz and 32 echoes in one segment was used to keep the echo train length short. With a matrix size of 64 × 64 (0.4 mm in-plane resolution), a set of 13, 1.5 mm slices could be obtained in 20 s.

Phantoms

Five or seven-tubes phantom, each tube (4.7 mm i.d.) containing 0–50 mM MC-P in phosphate buffered saline (PBS) as shown in Figure 2a, was used for measuring the in vitro T_1 relaxivity. The experimental conditions of SPGR and LL sequence were as follows: SPGR: TR = 75 ms, TE = 3 ms, FA = 45°, N_{EX} = 8, Scan time = 160 s, FOV = 3.2 × 3.2 cm, reconstructed image resolution = 256 × 256, slice thickness = 2.0 mm. Number of slices = 6. The LL T_1 mapping data was acquired by conventional gradient-echo MRI with TR = 10 s, TE 2.4 ms, FA = 20°, acquisition interval = 400 ms, number of time point = 20, and matrix size = 96 × 96.

Animal Experimental Design

Rats were anesthetized by isoflurane (2.0 %) in medical air (700 mL/min) and secured on a special holder by adhesive skin tape. A breathing sensor (SA Instruments, Inc., NY) was placed on the dorsal side of the rat. A non-magnetic temperature probe (FISO, Quebec, Canada) was used to monitor rectal temperature of the rats. The tail vein was cannulated for the injection of MC-P or 3CxP. The rat was then placed in the resonator, which was previously warmed up using a hot water cycling pad. The resonator unit including the rat was placed in the magnet bore. The MR measurements were started after the rat's core body temperature stabilized to 37°C. The rat body temperature was kept at 37 ± 1°C during experiments. Before making the measurements with the MC-P or 3CxP, images of the rat were taken with the parameters mentioned above. T_1-weighted images or T_1 maps were acquired continuously for 13 minutes, using SPGR or LL sequence. A solution of MC-P or CxP (1.5 μmol/g b.w.) was injected via tail vein cannulation, 2.0 min after starting the scan. To stop the blood flow immediately, 2 mL of KCl solution (2 mEq/mL) was injected 40 s after administration of MC-P and then continuously measured by SPGR till 13 min.

Surgical procedure of ischemia and reperfusion in rat

The intraluminal suture model was used for induction of focal cerebral ischemia, as formerly described by published procedure (Nagasawa and Kogure 1989). Briefly, rats were anesthetized with isoflurane using a nose cone. Anesthesia induction started with 4 % isoflurane carried by medical air and maintained by 2% isoflurane with medical air. Animal core body temperature will be maintained ~ 37 C using a water blanket. A 2 cm midline incision was made on anterior neck. The right common carotid artery (CCA), extra carotid artery (ECA), and internal carotid artery (ICA) were exposed with careful conservation of vagus nerve. The CCA and ECA were ligated and a suture was placed at the ICA. To block the origin of middle cerebral artery (MCA), a 4-0 nylon surgical thread was advanced into the ICA via a small incision. The left CCA was ligated with suture to complete the MCAO. After 1 hr of MCAO, normal blood flow was restored in the MCA by withdrawing the suture tip and the suture of the left CCA region. The rats were moved to the MR magnet 3 hr after reperfusion. Then MRI procedure was performed as described above.

Image Analysis

The MRI data were analyzed using the ImageJ software package (http://rsb.info.nih.gov/ij/). The T_1 of each pixel was calculated in two steps using a custom-written program running in Matlab (The MathWorks, Inc., Natick, MA, USA). First, the signal recovery of each pixel was fitted by the Levenburg–Marquardt nonlinear three-parameter curve-fitting algorithm. Then, the obtained parameters were used to resolve the dependency of the fitted T_1 on the flip-angle and acquisition interval to derive the actual T_1 (Chuang and Koretsky 2006). Semi-logarithmic plots of the time course of MRI signal change in the region of interest (ROI) were used for reduction rate calculation. ROI analysis was performed on multi-slice LL data using ImageJ. The concentration of MC-P was estimated by the LL T_1 maps using the relaxivity measured in the phantom study with the following equation:

$$[\text{MC-P}] = (R_1 - R_{10}) / \text{Relaxivity}$$

Statistical analysis was performed using StatView software Stat View 5.0, SAS Institute, Inc., Cary, NC, USA). All data are presented as mean ± SD.

Quantification of MC-P in Brain and Blood by EPR spectroscopy

MC-P dissolved in saline was injected in the tail vein of rats at a dose of 0.75 μmol/g body weight (5 μL/g). The concentration in the bolus solution was 150 mM. The blood was collected from retro-orbital sinus using heparinized tubes. The brain tissue was extracted 2,

5, 8 min after injection of MC-P and wet weight was determined. Blood or tissue samples were diluted or homogenized with four-fold volume for blood or three fold volume PBS for brain. The homogenate solution was mixed with ferricyanide solution (2 mM). The ferricyanide quantitatively oxidizes the hydroxylamaine produced as a result of *in vivo* reduction back to the oxidized form (Krishna *et al* 1992; Krishna *et al* 1996a; Krishna *et al* 1996b). The signal intensities of the 100 μL samples were immediately measured using a Varian E-9 X-band EPR spectrometer. The EPR spectrometer operating conditions were: modulation frequency, 100 kHz, Microwave power, 1 mW. Since there is linearity up to 2 mM between concentration and EPR signal height of MC-P (data not shown), EPR signal heights of homogenate mixtures were converted to the concentration using previously obtained standard curves with or without ferricyanide solution (100 μM - 2 mM). Finally, MC-P concentrations in the brain tissue and blood were calculated based on the dilution factor.

Results

Figure 2a (middle column) shows T_1 weighted images of phantom with various concentrations of MC-P acquired using the SPGR sequence. The MR signal intensity increased with concentration of MC-P up to 50 mM (Fig. 2b), with a linear response up to 5 mM. The intensity change (%) in the 5 mM MC-P tube was about 100 % compared to PBS (center tube). The T_1 maps of the phantom by the LL sequence are shown in figure 2a (right column). The T_1 values decreased depending on MC-P concentration from 2246 ms (0.5 mM) to 122 ms (50 mM), and the relaxation rates ($1/T_1$) increased linearly up to 50 mM (Fig. 2). The relaxivity of MC-P in PBS solution was measured to be 0. 16 s^{-1} mM^{-1} by the LL sequence.

To study the dynamics of the nitroxides in the brain, a T_1 weighted SPGR sequence was used. Using this technique, 6 slices (2 mm slice thickness) were obtained every 20 s with an image resolution of 125 μm. After injection of MC-P solution, the intensity in the rat head region immediately increased (green color). The increased signal intensity in the brain tissue was large compared to facial muscle (Fig. 3a). The maximum signal intensity change in the brain tissue after injection of MC-P was about 50 % compared to the pre-injection image (Fig. 3c). The signal intensity derived from MC-P (oxidized form, MRI visible) reached a maximum 30 s after injection, and the signal intensity decreased during the subsequent 6 min. On the other hand, 3CxP (cell-impermeable) didn't cause significant signal changes in the brain region although it has a similar in vitro relaxivity (0.17 s^{-1} mM^{-1}) as MC-P (Fig. 3b). The signal intensity in the cerebral cortex and thalamus increased by only 2.7 % during the measurement time and increased signal intensity plateaued for up to 10 min after injection of 3CxP (Fig. 3d). To check if blood flow affected MC-P reduction, blood flow was stopped by KCl injection 40 s after administration of MC-P. Respiration stopped (rats died) 15–20 s after KCl injection. MR signal intensity in brain decreased after enhancement by MC-P in a manner similar to that found for brain but slower than in animals with normal cerebral perfusion (Fig. 3e). The MC-P reduction rate ($k = 0.30 \pm 0.066$ min^{-1}) in the brain without flow was slower than in living rat brain ($k = 0.50 \pm 0.039$ min^{-1}), indicating that a fraction of the reduction of intensity enhancement might have been due to washout from the brain. Alternately a change in tissue redox upon death could explain these differences.

In ischemia-reperfusion (IR) treated group, all rats showed typical symptoms during ischemia, and all rats were alive after IR. The T_2 weighted MR images in IR group did not show any differences at this time (Fig.4a). However, significantly high intensity regions 24 hr after IR were observed (data not shown). The reduction rate of MC-P in the right hemisphere was significantly decreased compared to same region of sham rat brain (Fig. 4c).

Figure 5a shows the time course of quantitative T_1 maps before and after injection of MC-P. T_1 map data was obtained every 20 s with 13 slices (1.5 mm slice thickness) by the EPI-LL sequence. The T_1 maps clearly showed the difference of T_1 relaxation time between cerebral cortex and thalamus. The relaxation times in cerebral cortex and thalamus before injection were 1577 ± 19.9 and 1315 ± 11.9 ms, respectively (Fig. 5b). The T_1 of these regions rapidly decreased after injection of MC-P, and the minimum T_1s of cerebral cortex and thalamus region were 1034 ± 70.4 and 779 ± 70.2 ms, respectively. The recovery of T_1 in the cerebral cortex and thalamus showed similar trends. From the T_1 and in vitro relaxivity of MC-P (0.16 $mM^{-1}s^{-1}$), the concentration of MC-P at all time points in the ROI was calculated (Fig. 5c). The maximum concentration in cerebral cortex and thalamus 30 s after injection was 1.9 ± 0.35 and 3.0 ± 0.50 mM, respectively. The concentration was significantly higher in thalamus compared to cerebral cortex. This difference of concentration was observed up to 2 min after injection after which the concentration in those regions converged.

To confirm whether the concentration of MC-P determined by the MRI technique is reliable, an ex-vivo study using x-band EPR was carried out on the brain tissue for MC-P levels (Fig. 6). The oxidized form and total MC-P (oxidized + reduced form) levels were determined with or without ferricyanide solution respectively. The brain tissue MC-P level was 0.84 ± 0.035 mM at 2 min after MC-P injection (Fig. 6a). This was in agreement with the MRI data in the cerebral cortex (0.83 ± 0.107 mM) and in the thalamus (0.94 ± 0.086 mM). On the other hand, total MC-P level (oxidized + reduced form) was 1.57 ± 0.199 mM, suggesting that approximately half of MC-P was in the reduced form in the brain at this time point. At 8 min, most of MC-P was reduced (0.24 ± 0.107 mM), however total MC-P (reduced + oxidized) still remained (0.92 ± 0.092 mM).

The blood concentration at different time from 6 rats is shown in Fig. 6b. The oxidized form of MC-P followed similar kinetics as the brain, peaking at similar concentration and falling off at a similar rate. Total MC-P levels slowly decreased, and but MC-P was still present at 30 min (oxidized MC-P level: 0.33 ± 0.084 mM, total level: 1.04 ± 0.07 mM), suggesting that the clearance of MC-P from the blood was much slower than reduction detected in the brain.

Discussion

The results of present study demonstrate that cell-permeable and low molecular weight BBB permeable MRI contrast agent, MC-P, is useful for enhancing MRI intensity in the brain. Furthermore, dynamic contrast enhancement study with LL sequence allowed us to get rapid T_1 maps from the brain region before and after MC-P injection. This enabled determination of the MC-P concentration in brain regions assuming the in vivo relaxivity of MC-P as the same in vivo.

Previously, we reported that nitroxide radicals are useful in monitoring tumor redox status (Hyodo *et al* 2006; Matsumoto *et al* 2006). In the present study, the cell-permeable and highly lipophilic nitroxide, MC-P was tested in the brain as an imaging probe. The T_1 weighted MR signal intensity of MC-P showed linearity up to 5 mM (Fig. 2b), though it increased up to 50 mM. The relaxation rate ($1/T_1$) was linear up to 50 mM (Fig. 2c). Because the MC-P concentration in the thalamus region went up to approximately 3 mM, EPR spectral line broadening effect might compromise the accuracy of quantification as probes in EPR and Overhauser MRI, two commonly used techniques to monitor nitroxides. However, MRI is not affected by the EPR spectral line broadening, therefore, it can provide more accurate information on the concentration.

In the animal studies, MRI signal intensities in brain regions clearly increased up to 50 % after injection of MC-P, although there was no enhancement (~ 3 %) in the case of the cell- and BBB-impermeable nitroxide, 3CxP.Both agents have one unpaired electron, their molecular structures are very similar, and their relaxivities are similar (0.16 $mM^{-1\cdot}\ s^{-1}$ for MC-P; 0.17 $mM^{-1\cdot}\ s^{-1}$ for 3CxP). Thus the difference detected is most likely due to distribution of MC-P in the brain. MC-P is a highly lipophilic substance with a octanol-water partition coefficients (Po/w) of 14.4 (Miura *et al* 1997). In addition to lipophilicity, its low molecular weight (200) allows it to pass through the BBB. Therefore, SPGR signal intensity in the brain region increased after MC-P injection (Fig. 3a). On the other hand, Po/w of 3CxP is 0.002, and it is not cell-permeable except by active anion transport (Ichikawa *et al* 2006). As a result, the MR signal intensity in the brain increased by only 2.7 %. The ratio of maximum intensity change between MC-P and 3CxP is 18.5. This ratio was very similar to the blood volume in the brain. The brain blood value is about 5 ~ 10 % in the whole brain and the ratio to tissue is about 10 ~ 20 (Ladurner *et al* 1976; Mathew *et al* 1972; Rostrup *et al* 2005). These data suggest that MC-P distributed in whole brain tissue region after passing through the BBB.

The levels of 3CxP were stable in the blood for up to 13 min. Our previous paper showed that 3CxP displays slow pharmacokinetics compared to cell-permeable contrast agents and its reduction rate was attributed to its membrane permeability (Hyodo *et al* 2006). In addition, blood flow may contribute in nitroxide reduction in vivo. Therefore, MC-P reduction rate without blood flow was tested (Fig. 3e). Even though blood flow was stopped after injecting KCl solution, MC-P reduced in the brain. The reduction rate of MC-P without blood flow was 60 % compared with blood flow, suggesting that MC-P reduction represents reaction with intracellular reductants such as GSH, AsA and possibly free radicals in the intracellular compartment. It is also possible that, when animal died the brain redox status changed in a manner that showed the reduction of MC-P.

Monitoring of T_1s before and after injection of MC-P using LL sequence allowed the calculation of MC-P concentration in the brain (Fig. 5). Thirteen slices of brain T_1 maps with 1.5 mm slice thickness were obtained every 20 s, and monitored continuously up to 13 min (a representative slice is shown in Figure 5a). The T_1 values in the ROI were converted to MC-P concentration (Fig. 5c). The concentration determined by MRI was in agreement with the results measured from brain tissues and the blood concentration of the oxidized form of MC-P as determined ex-vivo from EPR (Fig. 6). Although there were about 0.5 mM oxidized form MC-P concentration at 10 min after injection, the total MC-P levels (nitroxide + hydroxylamine) was still around 1.2 mM, suggesting that the reduction from MC-P (oxidized, paramagnetic) to hydroxylamine (reduced, dismagnetic) was predominant compared to clearance and elimination from the brain tissue or blood.

Lowered reduction rate in the infarction area after ischemia and reperfusion were readily seen in the right hemisphere (Fig. 4) suggesting that post-ischemic reperfusion damage course induced elevated oxidative conditions in infarct region resulting in oxidative damage. Major antioxidants such as AsA (AsA #0) and GSH are efficient reducing substances in the brain and are found at millimoler levels (Rice and Russo-Menna 1998; Rice *et al* 2002). Low levels of these antioxidants have been implicated in neurological damage and stroke. Under normal physiological condition, neurological damages mediated by ROS can be prevented by the cellular antioxidant network. However, AsA levels decrease in the brain and rise sharply in extracellular fluid of the brain following severe ischemic hypoxia (Hillered *et al* 1988; Landolt *et al* 1992). The nitroxide radical by itself is also an antioxidant and can be used as an SOD mimic (Krishna *et al* 1996a). Tempol which is another cell permeable nitroxide has been used in a phase I clinical trial for the prevention of alopecia induced by whole brain radiotherapy (Metz *et al* 2004). Interestingly, in a tumor model,

Kuppsammy et al. demonstrated an increased rate of EPR signal decay of 3CP compared to normal tissue. This decay was decreased by pre-injection of a glutathione synthesis inhibitor, L-buthionine-S,R-sulfoximine (Kuppusamy *et al* 2002). These data suggest that MC-P effect on MRI signal intensity might enable monitoring of brain damage following alterations in levels of GSH. As a consequence, the BBB permeable nitroxide, MC-P may be useful as a MRI contrast agent to indicate a change in brain redox status. Furthermore MC-P might provide protection of brain due to tissue antioxidant properties.

Conclusion

The BBB-permeable MC-P has potential as a redox sensitive MRI contrast agent in brain. MRI intensity in brain was clearly enhanced after an injection of MC-P. Furthermore, the real time T_1 mapping by LL sequence allowed accurate monitoring of pharmacokinetic MC-P concentration changes with whole brain coverage. Such studies should be useful to evaluate brain redox status in brain oxidative diseases such as stroke, Alzheimer disease and other neurological disorders.

Reference

Anzai K, Saito K, Takeshita K, Takahashi S, Miyazaki H, Shoji H, Lee MC, Masumizu T, Ozawa T. Assessment of ESR-CT imaging by comparison with autoradiography for the distribution of a blood-brain-barrier permeable spin probe, MC-PROXYL, to rodent brain. Magn Reson Imaging. 2003; 21:765–772. [PubMed: 14559341]

Anzai K, Ueno M, Yoshida A, Furuse M, Aung W, Nakanishi I, Moritake T, Takeshita K, Ikota N. Comparison of stable nitroxide, 3-substituted 2,2,5,5-tetramethylpyrrolidine-N-oxyls, with respect to protection from radiation, prevention of DNA damage, and distribution in mice. Free Radic Biol Med. 2006; 40:1170–1178. [PubMed: 16545684]

Chuang KH, Koretsky A. Improved neuronal tract tracing using manganese enhanced magnetic resonance imaging with fast T(1) mapping. Magn Reson Med. 2006; 55:604–611. [PubMed: 16470592]

Crawley AP, Henkelman RM. A comparison of one-shot and recovery methods in T1 imaging. Magn Reson Med. 1988; 7:23–34. [PubMed: 3386519]

Erker L, Schubert R, Yakushiji H, Barlow C, Larson D, Mitchell JB, Wynshaw-Boris A. Cancer chemoprevention by the antioxidant tempol acts partially via the p53 tumor suppressor. Hum Mol Genet. 2005; 14:1699–1708. [PubMed: 15888486]

Hahn SM, Wilson L, Krishna CM, Liebmann J, DeGraff W, Gamson J, Samuni A, Venzon D, Mitchell JB. Identification of nitroxide radioprotectors. Radiat Res. 1992; 132:87–93. [PubMed: 1410280]

Hahn SM, Sullivan FJ, DeLuca AM, Krishna CM, Wersto N, Venzon D, Russo A, Mitchell JB. Evaluation of tempol radioprotection in a murine tumor model. Free Radic Biol Med. 1997; 22:1211–1216. [PubMed: 9098095]

Hahn SM, Krishna MC, DeLuca AM, Coffin D, Mitchell JB. Evaluation of the hydroxylamine Tempol-H as an in vivo radioprotector. Free Radic Biol Med. 2000; 28:953–958. [PubMed: 10802227]

Halliwell B. Oxidative stress and neurodegeneration: where are we now? J Neurochem. 2006; 97:1634–1658. [PubMed: 16805774]

He G, Samouilov A, Kuppusamy P, Zweier JL. In vivo imaging of free radicals: applications from mouse to man. Mol Cell Biochem. 2002; 234–235:359–367.

Hillered L, Persson L, Bolander HG, Hallstrom A, Ungerstedt U. Increased extracellular levels of ascorbate in the striatum after middle cerebral artery occlusion in the rat monitored by intracerebral microdialysis. Neurosci Lett. 1988; 95:286–290. [PubMed: 3226614]

Huang J, Agus DB, Winfree CJ, Kiss S, Mack WJ, McTaggart RA, Choudhri TF, Kim LJ, Mocco J, Pinsky DJ, Fox WD, Israel RJ, Boyd TA, Golde DW, Connolly ES Jr. Dehydroascorbic acid, a blood-brain barrier transportable form of vitamin C, mediates potent cerebroprotection in experimental stroke. Proc Natl Acad Sci U S A. 2001; 98:11720–11724. [PubMed: 11573006]

Hyodo F, Matsumoto K, Matsumoto A, Mitchell JB, Krishna MC. Probing the intracellular redox status of tumors with magnetic resonance imaging and redox-sensitive contrast agents. Cancer Res. 2006; 66:9921–9928. [PubMed: 17047054]

Ichikawa K, Sato Y, Kondo H, Utsumi H. An ESR contrast agent is transported to rat liver through organic anion transporter. Free Radic Res. 2006; 40:403–408. [PubMed: 16517505]

Keana JF, Pou S. Nitroxide-doped liposomes containing entrapped oxidant: an approach to the "reduction problem" of nitroxides as MRI contrast agents. Physiol Chem Phys Med NMR. 1985; 17:235–240. [PubMed: 3001795]

Koizumi J, Yoshida Y, Nakazawa T, Ooneda G. Experimental studies of ischemic brain edema. I A new experimental model of cerebral embolism in rats in which recirculation can be introduced in the ischemic area. Jpn J Stroke. 1986; 8:1–8.

Krishna MC, Grahame DA, Samuni A, Mitchell JB, Russo A. Oxoammonium cation intermediate in the nitroxide-catalyzed dismutation of superoxide. Proc Natl Acad Sci U S A. 1992; 89:5537–5541. [PubMed: 1319064]

Krishna MC, Russo A, Mitchell JB, Goldstein S, Dafni H, Samuni A. Do nitroxide antioxidants act as scavengers of O2-. or as SOD mimics? J Biol Chem. 1996a; 271:26026–26031. [PubMed: 8824242]

Krishna MC, Samuni A, Taira J, Goldstein S, Mitchell JB, Russo A. Stimulation by nitroxides of catalase-like activity of hemeproteins. Kinetics and mechanism. J Biol Chem. 1996b; 271:26018–26025. [PubMed: 8824241]

Kuppusamy P, Chzhan M, Wang P, Zweier JL. Three-dimensional gated EPR imaging of the beating heart: time-resolved measurements of free radical distribution during the cardiac contractile cycle. Magn Reson Med. 1996; 35:323–328. [PubMed: 8699943]

Kuppusamy P, Li H, Ilangovan G, Cardounel AJ, Zweier JL, Yamada K, Krishna MC, Mitchell JB. Noninvasive imaging of tumor redox status and its modification by tissue glutathione levels. Cancer Res. 2002; 62:307–312. [PubMed: 11782393]

Ladurner G, Zilkha E, Iliff D, du Boulay GH, Marshall J. Measurement of regional cerebral blood volume by computerized axial tomography. J Neurol Neurosurg Psychiatry. 1976; 39:152–158. [PubMed: 1262889]

Landolt H, Lutz TW, Langemann H, Stauble D, Mendelowitsch A, Gratzl O, Honegger CG. Extracellular antioxidants and amino acids in the cortex of the rat: monitoring by microdialysis of early ischemic changes. J Cereb Blood Flow Metab. 1992; 12:96–102. [PubMed: 1727146]

Lee MC, Shoji H, Miyazaki H, Yoshino F, Hori N, Toyoda M, Ikeda Y, Anzai K, Ikota N, Ozawa T. Assessment of oxidative stress in the spontaneously hypertensive rat brain using electron spin resonance (ESR) imaging and in vivo L-Band ESR. Hypertens Res. 2004; 27:485–492. [PubMed: 15302985]

Liaw WJ, Chen TH, Lai ZZ, Chen SJ, Chen A, Tzao C, Wu JY, Wu CC. Effects of a membrane-permeable radical scavenger, Tempol, on intraperitoneal sepsis-induced organ injury in rats. Shock. 2005; 23:88–96. [PubMed: 15614137]

Longa EZ, Weinstein PR, Carlson S, Cummins R. Reversible middle cerebral artery occlusion without craniectomy in rats. Stroke. 1989; 20:84–91. [PubMed: 2643202]

Mariani E, Polidori MC, Cherubini A, Mecocci P. Oxidative stress in brain aging, neurodegenerative and vascular diseases: an overview. J Chromatogr B Analyt Technol Biomed Life Sci. 2005; 827:65–75.

Mathew NT, Meyer JS, Bell RL, Johnson PC, Neblett CR. Regional cerebral blood flow and blood volume measured with the gamma camera. Neuroradiology. 1972; 4:133–140. [PubMed: 4670711]

Matsumoto K, Hyodo F, Matsumoto A, Koretsky AP, Sowers AL, Mitchell JB, Krishna MC. High-resolution mapping of tumor redox status by magnetic resonance imaging using nitroxides as redox-sensitive contrast agents. Clin Cancer Res. 2006; 12:2455–2462. [PubMed: 16638852]

Metz JM, Smith D, Mick R, Lustig R, Mitchell J, Cherakuri M, Glatstein E, Hahn SM. A phase I study of topical Tempol for the prevention of alopecia induced by whole brain radiotherapy. Clin Cancer Res. 2004; 10:6411–6417. [PubMed: 15475427]

Miura Y, Anzai K, Takahashi S, Ozawa T. A novel lipophilic spin probe for the measurement of radiation damage in mouse brain using in vivo electron spin resonance (ESR). FEBS Lett. 1997; 419:99–102. [PubMed: 9426228]

Muir KW, Buchan A, von Kummer R, Rother J, Baron JC. Imaging of acute stroke. Lancet Neurol. 2006; 5:755–768. [PubMed: 16914404]

Nagasawa H, Kogure K. Correlation between cerebral blood flow and histologic changes in a new rat model of middle cerebral artery occlusion. Stroke. 1989; 20:1037–1043. [PubMed: 2756535]

Raichle ME, Mintun MA. Brain Work and Brain Imaging. Annu Rev Neurosci. 2006

Rice ME, Russo-Menna I. Differential compartmentalization of brain ascorbate and glutathione between neurons and glia. Neuroscience. 1998; 82:1213–1223. [PubMed: 9466441]

Rice ME, Forman RE, Chen BT, Avshalumov MV, Cragg SJ, Drew KL. Brain antioxidant regulation in mammals and anoxia-tolerant reptiles: balanced for neuroprotection and neuromodulation. Comp Biochem Physiol C Toxicol Pharmacol. 2002; 133:515–525. [PubMed: 12458180]

Rostrup E, Knudsen GM, Law I, Holm S, Larsson HB, Paulson OB. The relationship between cerebral blood flow and volume in humans. Neuroimage. 2005; 24:1–11. [PubMed: 15588591]

Samuni AM, DeGraff W, Krishna MC, Mitchell JB. Cellular sites of H2O2-induced damage and their protection by nitroxides. Biochim Biophys Acta. 2001; 1525:70–76. [PubMed: 11342255]

Sano H, Matsumoto K, Utsumi H. Synthesis and imaging of blood-brain-barrier permeable nitroxyl-probes for free radical reactions in brain of living mice. Biochem Mol Biol Int. 1997; 42:641–647. [PubMed: 9247722]

Yamada KI, Kuppusamy P, English S, Yoo J, Irie A, Subramanian S, Mitchell JB, Krishna MC. Feasibility and assessment of non-invasive in vivo redox status using electron paramagnetic resonance imaging. Acta Radiol. 2002; 43:433–440. [PubMed: 12225490]

Yokoyama H, Itoh O, Aoyama M, Obara H, Ohya H, Kamada H. In vivo temporal EPR imaging of the brain of rats by using two types of blood-brain barrier-permeable nitroxide radicals. Magn Reson Imaging. 2002; 20:277–284. [PubMed: 12117610]

Zimmermann C, Winnefeld K, Streck S, Roskos M, Haberl RL. Antioxidant status in acute stroke patients and patients at stroke risk. Eur Neurol. 2004; 51:157–161. [PubMed: 15073440]

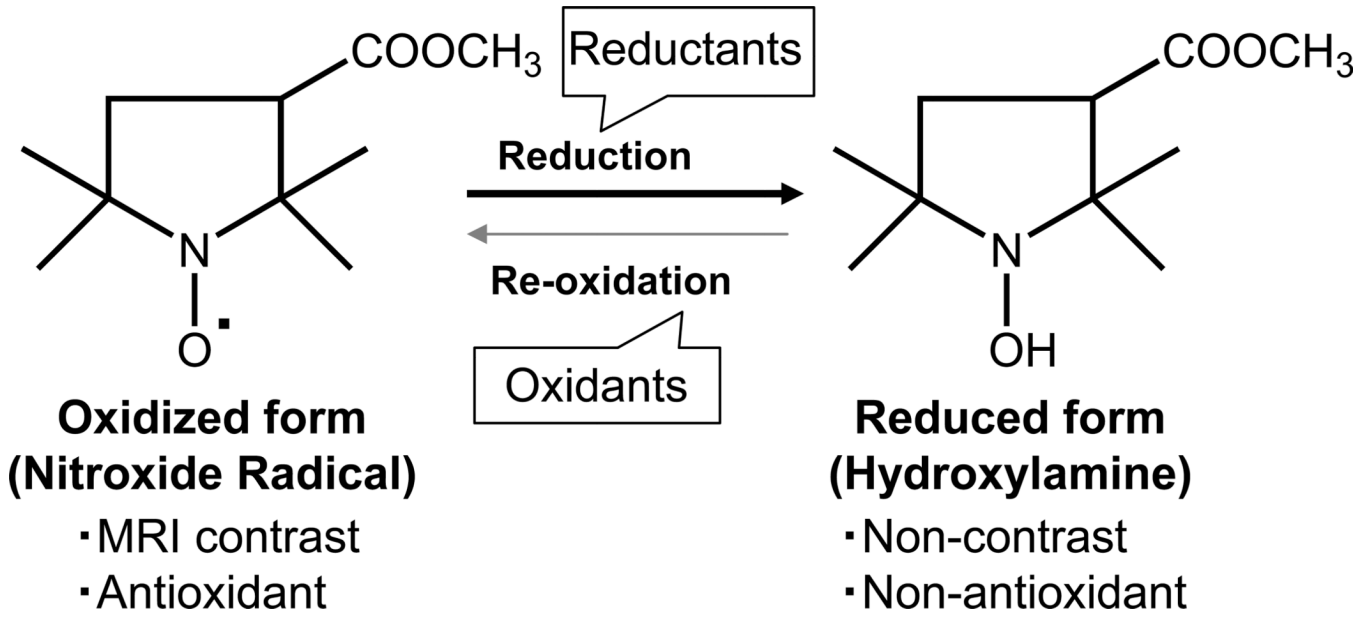

Figure 1.
Reversible one-electron reduction / oxidation showing the interconversion and the molecular structure of MC-P. Left structure is radical form of MC-P. Right structure is reduced form (hydroxylamine) of MC-P

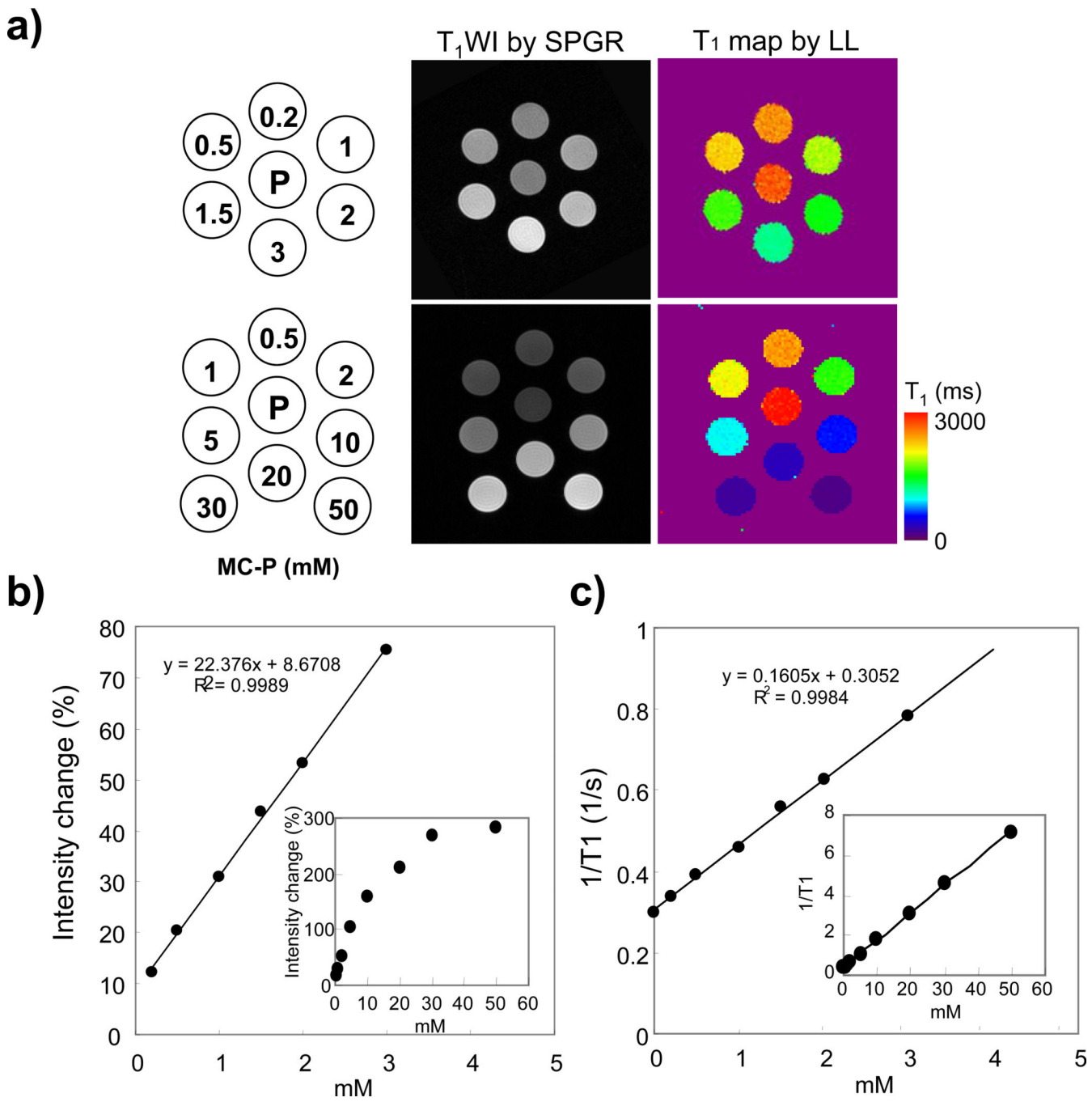

Figure 2.

MR images of MC-P phantom by SPGR and LL sequences. a) Schematics of the MC-P phantom (Left column) and T_1 weighted SPGR images (middle column) and T_1 maps (right column) calculated from LL sequence. The center phantom was filled with PBS. MC-P was dissolved in saline. b) MR signal intensity change of MC-P phantom as a function of concentration from 0.2 mM to 50 mM. Signal intensity change (%) was calculated based on PBS phantom intensity. c) Relaxation rate ($1/T_1$) of MC-P as a function of concentration. MRI parameters of SPGR and LL sequence are: **SPGR**: TR = 75 ms, TE = 3 ms, FA = 45°, N_{EX} = 8, Scan time = 160 s, FOV = 3.2 × 3.2 cm, reconstructed image resolution = 256 × 256, slice thickness = 2.0 mm, number of slices = 6. **LL sequence** The LL T_1 mapping data

was acquired by conventional gradient-echo with TR = 10 s, TE = 2.4 ms, FA = 20°, acquisition interval = 400 ms, number of time point = 20, and matrix size = 96 × 96.

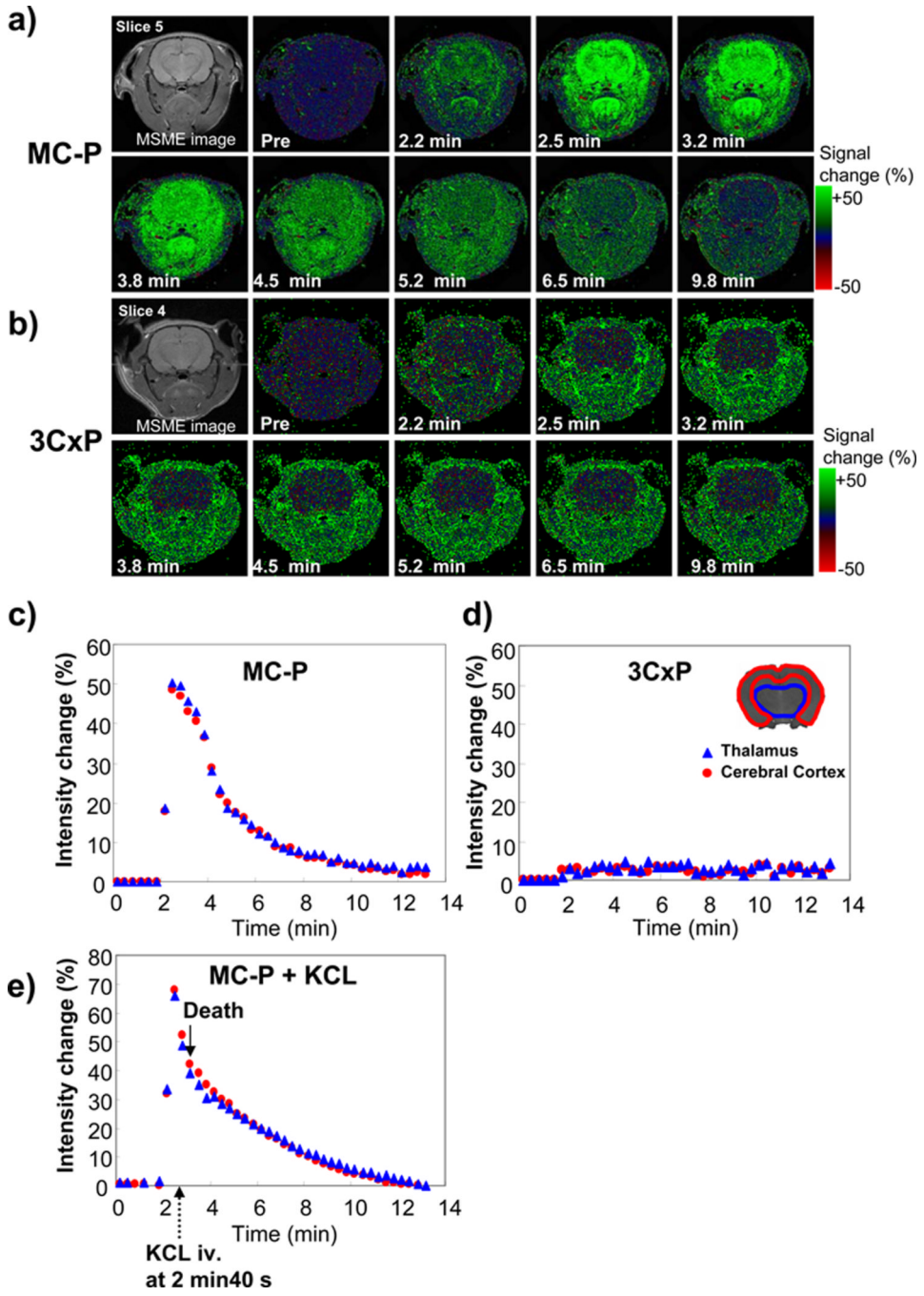

Figure 3.

Time-course SPGR MR images of rat head region after injection of a) MC-P (cell-permeable) and b) 3CxP (cell-impermeable). Contrast agents were injected 2 min after MR scan was started. 60 serial images were obtained in 20 min. T_2-weighted spin echo images (MSME image) were obtained before SPGR scan. SPGR MR parameters were as follows: image resolution was 256 × 128, zero-filled to 256 × 256 (0.125 mm resolution), FOV was 3.2 × 3.2 cm, slice thickness was 2.0 mm and 0.2 mm gap. Number of slices was 6. Green color shows MR signal intensity increased percentage (%) from the pixel of the pre-injection image. The time courses of intensity change of c) MC-P and d) 3CxP in the ROI of cerebral cortex (red color) and thalamus (blue color) are shown. e) Intensity change of MC-P without

blood flow is shown. KCl (2 mL) was injected 40 s after MC-P injection and rats died within 20 s.

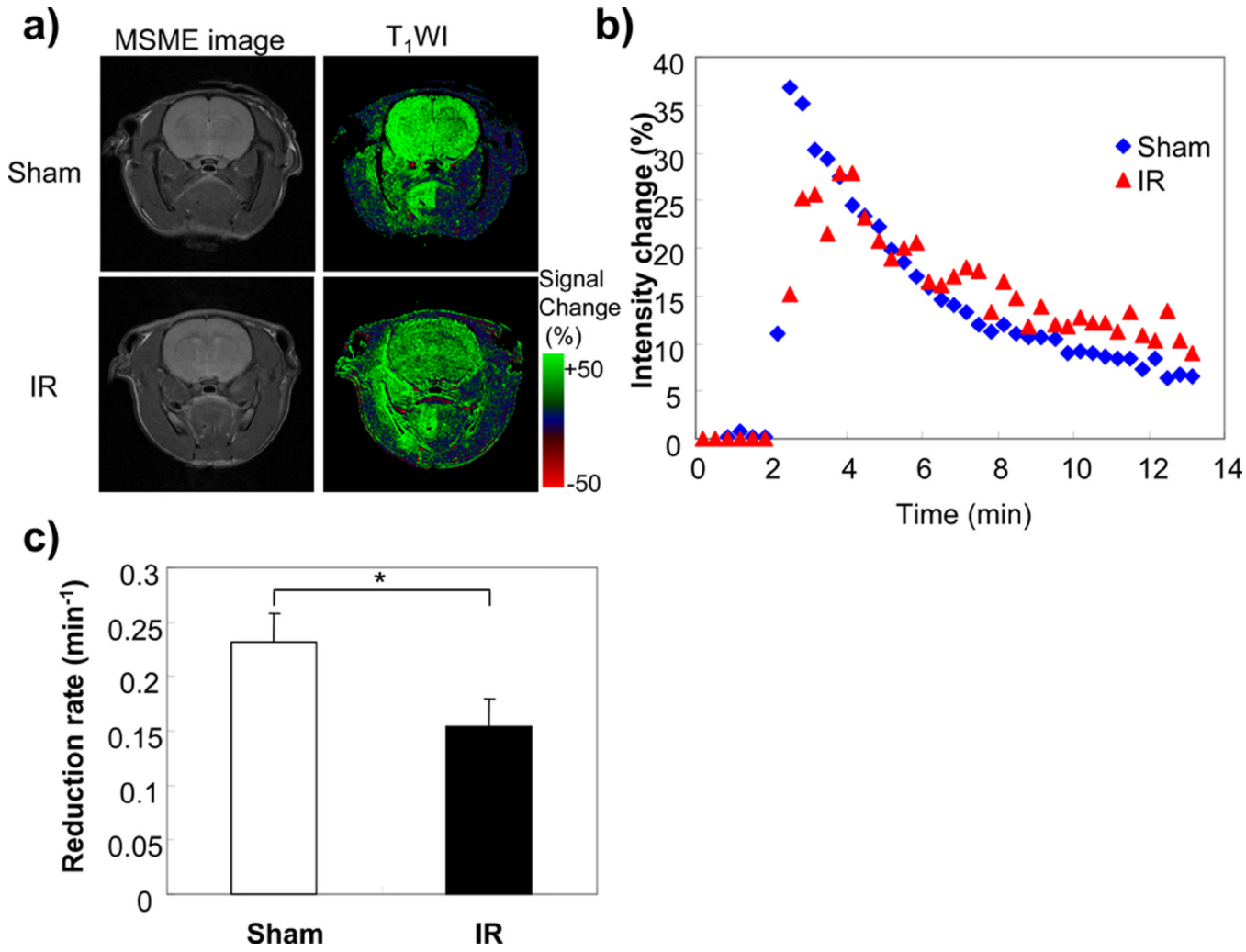

Figure 4.

Redox MR imaging of rat brain after ischemia and reperfusion (IR). a) T_2 weighted MR image and T_1 weighted MR image of sham and IR treated rats after MC-P injection. b) Intensity change of right hemisphere in the T_1 weighted MR images after MC-P injection. C) Reduction rate of right hemisphere in sham and IR treated rats. The data was averaged four animals. Error bars are SD. * $p < 0.01$, The significant difference between sham and IR rats by t-test.

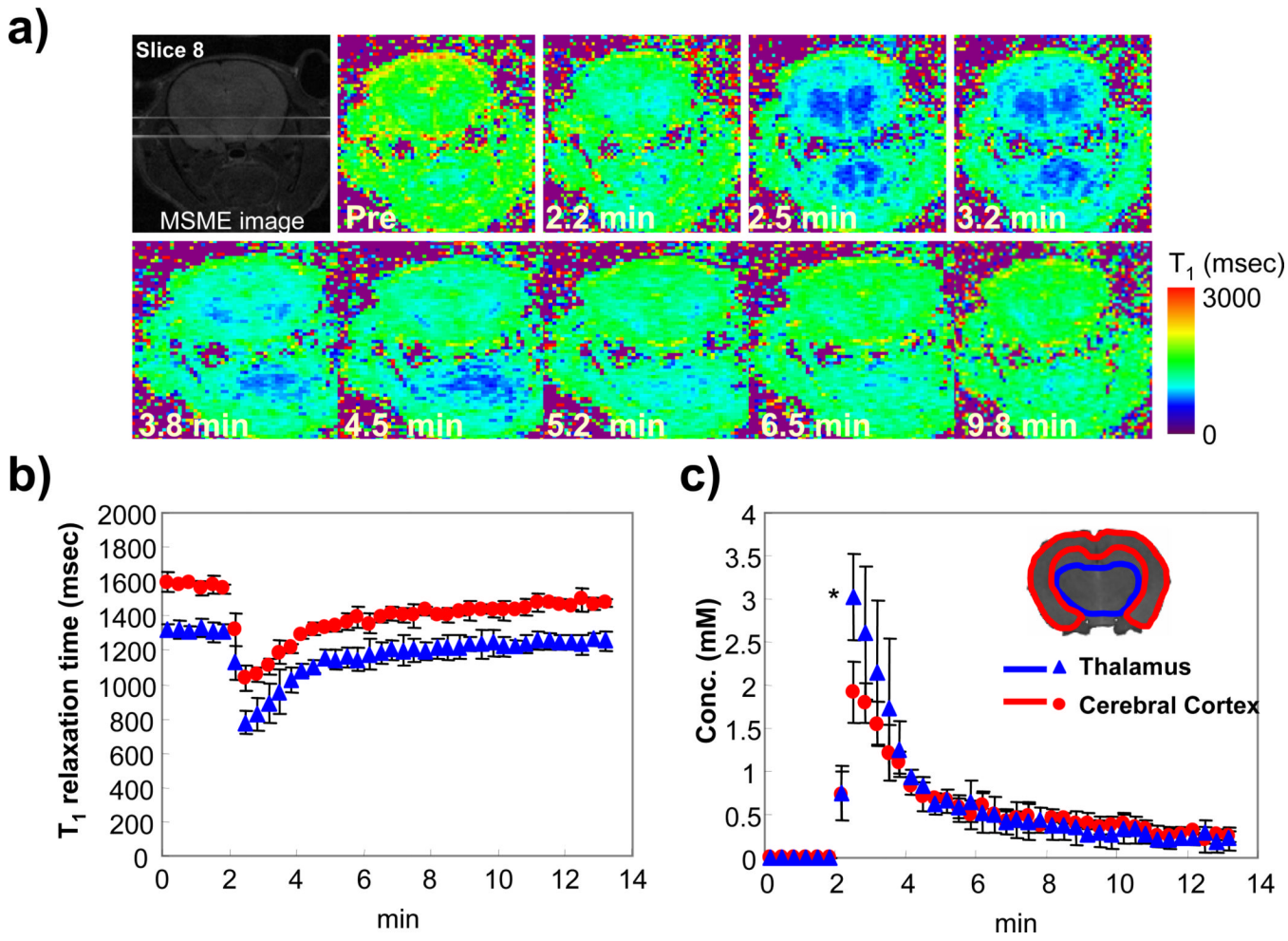

Figure 5.

Dynamic T_1 maps of rat head region after MC-P injection acquired by LL sequence. a) Time-course T_1 maps of rat head region after MC-P injection. Multi-slice LL data were acquired every 20 s by segmented EPI with TR = 10 s, TE 6.7 ms, FA = 20°, acquisition interval = 400 ms, and number of time point = 20. Slice thickness was 1.5 mm. The changes of b) T_1 and c) MC-P concentration in cerebral cortex and thalamus region were shown. The MC-P concentration was calculated from T_1 using equation shown in method section. Error bar is standard deviation (± SD, number of experiment was 3). * $p < 0.01$, The significant difference of maximum concentration of MC-P between cerebral cortex and thalamus by t-test.

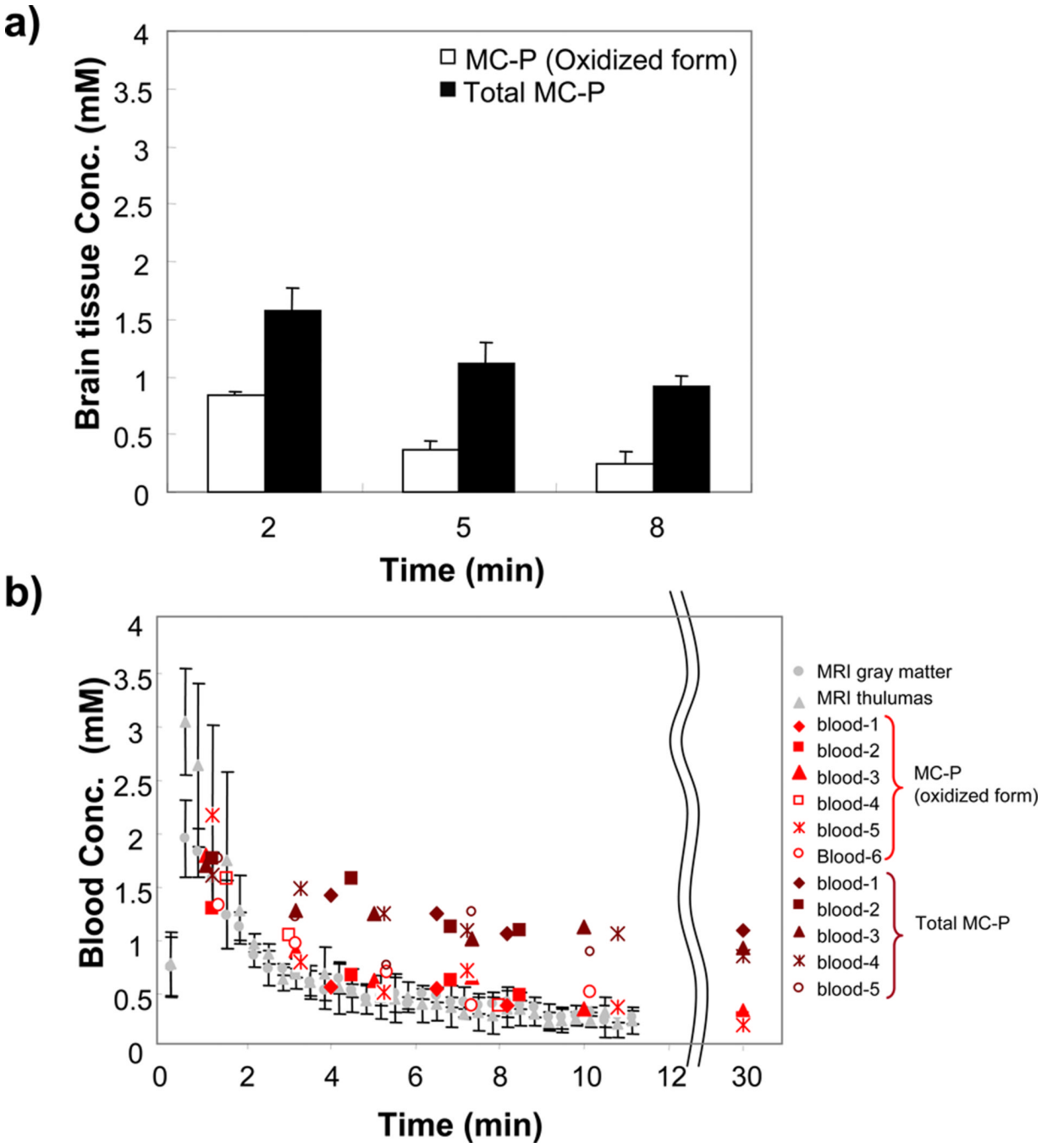

Figure 6.

The quantification of oxidized and total (oxidized + reduced) MC-P in brain tissue and blood using x-band EPR. a) The concentration change of oxidized (white bar) and total (black bar) MC-P in brain tissue (N = 4). b) Time course change of blood concentration of oxidized (Hillered *et al*) and total MC-P (brown). Gray color shows concentration change from the MRI same as in figure 5c. Blood was collected from eyeground using heparinized capillary (N = 6).